3D-TDOA Localization Using Airborne Sensors: A Comparative Algorithmic Study

Suman Agrawal
DSP (DRDO)
Hyderabad, TS

Madhura Barshikar
DSP (DRDO)
Hyderabad, TS

doi: https://doi.org/10.37285/bsp.SACAD2025.41

Abstract:
Time Difference of Arrival (TDOA)-based localization using airborne sensors has gained significant attention for tracking ground-based passive RF emitters, particularly in surveillance and defence operations. As multiple algorithms have been developed for TDOA geolocation, it becomes essential to evaluate their trade-offs in terms of localization accuracy and computational efficiency. This work presents a comparative study of several commonly used TDOA methods under varying operational scenarios. Special emphasis is placed on how factors such as the number of sensors, their spatial configuration, and their altitude influence geolocation performance. By integrating sensor height into the analysis, this study extends traditional 2D approaches to a more realistic 3D model, offering deeper insights into practical deployment using airborne platforms.

Key Words: Airborne sensors, Time Difference of Arrival (TDOA), Formation Flying, Maximum Likelihood, Root Mean Square Error

I. INTRODUCTION

Time Difference of Arrival (TDOA) has been widely adopted for the passive localization of signal emitters, especially in military and aerospace domains. Given its critical role in applications such as navigation, aviation, electronic warfare, and long-range surveillance, it is essential to understand the key factors that influence its localization accuracy. Among the various geolocation techniques, hyperbolic positioning is one of the most commonly employed approaches. It estimates the source location by measuring the time differences in signal arrival between several spatially distributed sensors and a reference sensor.

Estimating the precise location of a signal source is inherently challenging due to the nonlinear nature of the measurement equations involved. To address this, a range of localization algorithms have been developed, including both non-iterative closed-form solutions and iterative optimization-based approaches. While iterative methods often offer improved accuracy, they come with increased computational complexity. Therefore, this study focuses on evaluating the performance of two commonly used non-iterative algorithms under controlled conditions to assess their practicality and effectiveness.

Monte Carlo simulations are employed to repeat the localization process multiple times, thereby providing statistically meaningful performance estimates in terms of localization error. To further improve the estimation accuracy, a Maximum Likelihood Estimator (MLE) is applied as a post-processing step.

In addition, this work investigates how localization accuracy is influenced by the number of sensors, their spatial arrangement, and especially their operating altitude. Multiple sensor geometries are simulated within realistic airborne deployment scenarios, using airborne sensors placed at various altitudes. The performance is quantitatively evaluated using Root Mean Square Error (RMSE) and the Cramér-Rao Lower Bound (CRLB) as primary accuracy metrics.

A wide range of recent research has contributed to the advancement of Time Difference of Arrival (TDOA)–based localization across various application scenarios and sensor configurations. Early foundational techniques, such as the estimator proposed by Chan and Ho [6], remain influential, while comparative evaluations involving TDOA, Angle of Arrival (AOA), and Received Signal Strength (RSS) methods have helped establish performance benchmarks under diverse conditions [3], [4], [7]. More recent investigations have incorporated neural networks for signal interpretation [5], explored deployment in ultra-wideband (UWB) systems [8], and examined implementation over communication protocols like LoRaWAN [9]. Enhancements in localization accuracy through sensor placement strategies and optimal network geometries have also been studied extensively [1], [2], [10], [13]. Additional efforts have focused on improving system robustness through intelligent sensor selection [13], regularization techniques such as Tikhonov's method [14], and mitigation of time synchronization vulnerabilities [11]. Furthermore, integrated approaches combining TDOA with AOA and RSS measurements have shown significant potential in challenging environments involving sparse or heterogeneous sensor networks [3], [15]. Together, these contributions reflect a strong and growing interest in developing reliable, precise, and application-ready TDOA localization frameworks.

The paper is organized as follows: Section I - Mathematical Modeling, Section II - Simulation Scenario, Section III - Simulation Results, Section IV - Conclusions, followed by Acknowledgment and References.

II. MEASUREMENT MODEL

Let the unknown position of the signal emitter (source) be represented as a 3-dimensional vector:

$$\mathrm{x} = [\mathrm{x}, \mathrm{y}, \mathrm{z}]^{\mathrm{T}}$$

Assume there are airborne sensors deployed, each with a known position. The location of the sensor is denoted by:

$$s_i = [x_i, y_i, z_i]^T$$

A. Range and TDOA definition

The Euclidean distance (or range) from the source to the sensor is given by:

$$r_i(x) = ||x - s_i||$$

$$r_i(x) = \sqrt{((x - x_i)^2 + (y - y_i)^2 + (z - z_i)^2)}$$

The Time Difference of Arrival (TDOA) between sensor and the reference sensor (sensor 1) is defined as:

$$\tau_i(x) = r_i(x) - r_1(x)$$

Stacking all TDOA values into a vector, the TDOA observation vector is expressed as:

The TDOA vector $\tau(x) \in R^{\{N-1\}}$ is:

$$\tau(x) = [r_2(x) - r_1(x), r_3(x) - r_1(x), \ldots, r_N(x) - r_1(x)]^T$$

B. Noise Modelling

Assume the measured TDOAs are corrupted by additive Gaussian noise. The noise vector is modeled as:

$$\eta \sim N(0, \sigma_t^2 I).$$

The measured TDOA vector is then given by:

$$\tau_{meas} = \tau(x) + \eta$$

Multiplying both sides by the signal propagation speed , the time errors are converted to range errors:

$$\varepsilon = c\eta \sim N(0, \sigma^2 I)$$

where $\sigma = c\sigma_t$

C. Linearization of the TDOA Model

Due to the nonlinearity of the TDOA function , we linearize it around an initial estimate using a first-order Taylor series approximation:
Linearize $\tau(x)$ about an initial guess x_0:

$$\tau(x) \approx \tau(x_0) + H(x_0)(x - x_0)$$

Where, $H \in R^{\{(N-1)\times 3\}}$ is the Jacobian matrix of partial derivatives of the TDOA vector with respect to the source position:

$$h_i = \partial\tau_i / \partial x = \frac{(x - s_i)}{r_i} - \frac{(x - s_1)}{r_1}$$

Thus,

$$H = [h_2; h_3; \ldots; h_N]$$

D. Least Square Estimation

Using the linearized model, the source position can be estimated using the Least Squares (LS) method as follows:

$$\hat{x} = x_0 + (H^T H)^{\{-1\}} H^T (\tau_{meas} - \tau(x_0))$$

E. Estimation Covariance

The covariance matrix of the estimation error is given by:

$$Cov(\hat{x}) = \sigma^2 (H^T H)^{\{-1\}}$$

This matrix characterizes the uncertainty in the position estimate due to measurement noise.

F. Geometric Delusion of Precision (GDOP)

To evaluate the impact of sensor geometry on localization accuracy, the Geometric Dilution of Precision (GDOP) is defined as:

$$GDOP = \sqrt{(trace((H^T H)^{-1}))}$$

If $Q = (H^T H)^{-1}$ has diagonal entries $\sigma_x^2, \sigma_y^2, \sigma_z^2$, then:

$$GDOP = \sqrt{(\sigma_x^2 + \sigma_y^2 + \sigma_z^2)}$$

G. Root Mean Square Error (RMSE)

The Root Mean Square Error (RMSE) represents the expected Euclidean error between the estimated and actual source positions:

$$RMSE = \sqrt{\left(E\left[||\hat{x} - x||^2\right]\right)} = \sqrt{\left(trace\left(Cov(\hat{x})\right)\right)}$$

Substituting from earlier, we obtain:

$$RMSE = \sigma * GDOP = c * \sigma_t * GDOP$$

This expression shows that the RMSE is directly proportional to the timing noise and is strongly influenced by sensor geometry via GDOP.

III. SIMULATION SCENARIO

This study presents a simulation-based evaluation of TDOA localization using a four-sensor airborne network configured in three geometric layouts: square, triangular, and cross. The target is modeled as a stationary, ground-based radio frequency (RF) emitter, while the airborne sensors are positioned at varying altitudes to reflect realistic deployment conditions. The RF emitter is defined using operational parameters representative of real-world defense and aerospace surveillance systems. These values, summarized in Table I, were carefully selected to ensure the simulation environment closely aligns with practical application scenarios.

Table 1. Transmission Parameters for Ground-based Emitter

Transmission Parameters	Values
Frequency Band	2 GHz
SNR	20 dB
Sampling Rate	1.5 GHz
Mode	Continuous Wave
Power	3 KW

To simulate realistic signal reception conditions, Gaussian timing noise with a standard deviation equivalent to 10 ns was introduced across all sensors. This accounts for synchronization errors, hardware imperfections, and environmental factors. The noise translates into range errors, affecting the accuracy of geolocation. To address this, a Maximum Likelihood Estimator (MLE) was applied as a refinement step after initial position estimation.

Among several non-iterative TDOA localization techniques tested, the Chan-Ho and Fang methods showed superior performance in terms of accuracy and stability. These two algorithms were selected for detailed comparison across all sensor geometries and altitudes. Further simulations were conducted using the best-performing geometry to analyze the effect of increasing the number of sensors and spatial separation. This holistic evaluation helped identify the optimal configuration for achieving high-precision TDOA-based localization using airborne sensor networks.

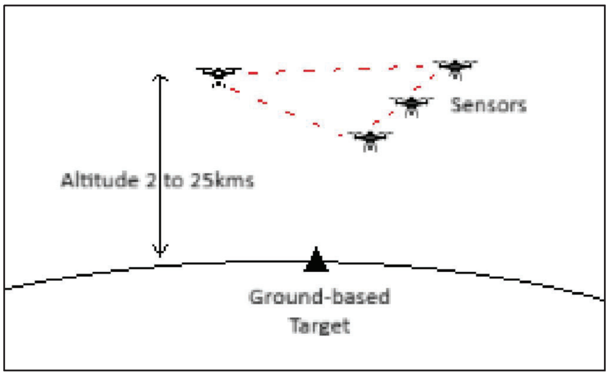

Fig.1. Formation flying in airborne

A figure 2 shows the illustration *of airborne TDOA-based localization geometry.* The figure depicts a typical airborne TDOA sensor deployment, where four sensors are mounted on aerial platforms operating at altitudes ranging from 2 km to 25 km above the Earth's surface. The sensors are arranged in a triangular configuration to ensure spatial diversity and minimize geometric dilution of precision (GDOP). A ground-based target emitter transmits a signal that is received by all sensors at slightly different times due to varying propagation paths. These time differences of arrival (TDOA) are then processed to estimate the target's position using multilateration. The variable altitude enables analysis of how vertical separation between the sensors and the target influences localization accuracy, coverage area, and CRLB-based performance limits.

The geometry of the sensor network plays a pivotal role in determining the accuracy and reliability of TDOA-based geolocation. Well-spread configurations help reduce Geometric Dilution of Precision (GDOP), leading to lower estimation errors. For instance, planar or collinear arrangements can result in ambiguous or elongated error ellipses, while properly spaced 3D geometries enable stronger triangulation of the emitter's position. In defense and aerospace operations, where the emitter may be hostile or concealed, the ability to deploy sensors in optimal configurations is critical for fast and precise localization. The chosen geometries in this study are representative of realistic aerial surveillance patterns, and the comparison helps determine which layout offers the best trade-off between spatial coverage, accuracy, and deployment feasibility.

Table 2. Coordinates of Geometries

Sensor Geometry	Coordinates (in kms)
Square	(-50,-50), (50,-50), (50,50), (-50,50)
Triangle	(0,-50), (50,50), (-50,50), (0,50)
Trapezoid	(25, -75), (50,75), (-50,-50), (-50,50)

Table 2 lists the planar coordinates for the three sensor geometries—square, triangle, and Trapezoid used in this study. Each configuration includes four airborne sensors positioned at a fixed altitude, while the target emitter remains on the ground. These geometries were selected to assess how spatial arrangement impacts the performance of TDOA-based localization.

The evaluation focuses on two key performance metrics: Root Mean Square Error (RMSE) and Geometric Dilution of Precision (GDOP). RMSE quantifies the average localization error under noise, with lower values indicating higher accuracy. In contrast, GDOP reflects the geometric quality of the sensor layout alone independent of noise or signal strength being influenced by factors like spacing, symmetry, and coverage. Lower GDOP values correspond to stronger geometric configurations. All results are based on simulations consistent with the mathematical models presented earlier.

IV. SIMULATION RESULT

Among the various non-iterative closed-form algorithms implemented, only the most accurate and computationally efficient ones were selected for comparison. The corresponding results are presented below.

a. Geometry Analysis

In this study, simulations were conducted over more than ten distinct four-sensor spatial arrangements to evaluate their impact on localization accuracy. Among these, the square, triangular, and cross-shaped configurations exhibited comparatively superior performance and were thus selected for in-depth analysis. The evaluation was employed with all sensors positioned at a fixed altitude of 25 km and the target emitter located at origin.

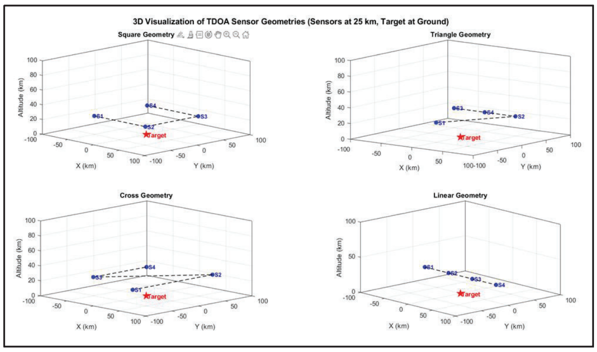

Fig 2: 3D visualization of four-sensor TDOA geometries at 25 km altitude showing how spatial configuration influences localization accuracy.

Figures 2 illustrate the spatial placement of four airborne TDOA sensors in various geometries — including square, triangular, trapezoidal, and linear layouts — within a 3D coordinate system. In all cases, the sensors are positioned at a fixed altitude of 25 km, while the target emitter is assumed to be located at the origin, representing a ground-based source. These configurations provide a clear visual understanding of how spatial arrangement influences TDOA measurements and the resulting hyperbolic intersection surfaces used for localization.

The geometry of the sensor network plays a decisive role in determining localization accuracy and robustness. Well-spread sensor placements minimize the Geometric Dilution of Precision (GDOP), leading to tighter error ellipses and reduced estimation uncertainty. In contrast, planar or collinear configurations may yield ambiguous or elongated error regions due to poor geometric diversity. The comparative analysis of these geometries, evaluated through CRLB-based performance metrics, highlights that properly distributed 3D arrangements—such as triangular or square layouts—offer superior accuracy and spatial coverage. At an altitude of 25 km, these configurations emulate realistic airborne or stratospheric platforms used in defence and surveillance operations, where precise emitter localization is essential for mission success. The accuracy metrics, including Root Mean Square Error (RMSE) and Geometric Dilution of Precision (GDOP), for these configurations are summarized in Table 3.

Table 3: Accuracy values for different geometries

Geometry	RMSE (m)	GDOP
Square	85.9953	101.4824
Triangle	74.4295	241.3920
Trapezoid	248.0498	446.5784

As observed from Table 3, the triangular sensor configuration achieves the lowest RMSE, indicating superior localization accuracy compared to other geometries. Although the square formation exhibits slightly lower GDOP due to its symmetric structure, the triangular layout offers a more favorable accuracy–geometry trade-off. The trapezoidal configuration performs comparatively poorer in both metrics. Hence, the triangular geometry is identified as the most effective arrangement for subsequent TDOA simulations and performance evaluations.

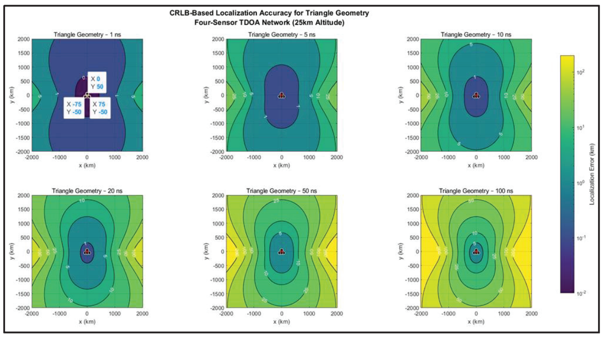

Fig.3. CRLB-Based Localization Accuracy for triangular Four-Sensor Airborne TDOA Network for 25 km Altitude

The CRLB contour plots for the triangular sensor configuration illustrate how localization precision varies with increasing timing uncertainty at orbital altitude. At low noise levels (1–10 ns), the region enclosed by the three vertices exhibits compact and nearly symmetric contours, indicating sub-kilometer accuracy near the centroid of the formation. As the timing error grows beyond 20 ns, the contours expand and gradually lose symmetry, revealing sensitivity degradation along the open edges of the triangle. This trend becomes more pronounced for 50 ns and 100 ns, where the error region extends over several hundred kilometers. The results confirm that although the triangular layout maintains balanced coverage, its localization performance at 25 km altitude is strongly constrained by timing precision, emphasizing the need for sub-10 ns synchronization for reliable satellite-based emitter geolocation.

b. Algorithm Analysis

The Root Mean Square Error (RMSE) values obtained for the Chan-Ho and Fang localization algorithms, evaluated under a four-sensor triangular configuration with sensors placed at an altitude of 25 km and the terrestrial target positioned at origin, are found to be 74.42 meters and 76.24 meters, respectively. These results demonstrate that both algorithms perform with comparable accuracy in this specific airborne geometry. However, the Chan-Ho algorithm yields a marginally lower RMSE, indicating slightly superior localization performance. Due to its improved accuracy and computational simplicity, the Chan-Ho method was selected as the preferred estimator for subsequent analysis and simulation scenarios in this study.

c. Altitude-based analysis for triangle geometry

In this section, the performance analysis is focused exclusively on the triangular sensor geometry, which was previously identified as the most accurate configuration based on RMSE evaluation. To investigate the impact of sensor altitude and algorithm selection on localization accuracy, the altitude of the airborne sensor platform is systematically varied from 2 km to 20 km. For each altitude level, RMSE values are computed using both the Chan-Ho and Fang algorithms across two distinct target positions. This setup enables a comparative assessment of how changes in vertical sensor placement influence estimation accuracy under different algorithmic approaches and target locations.

Table 4: Accuracy values for different algorithms for different altitudes

Altitude (km)	RMSE (m) at 20ns			
	(0,0,0)		(40, 60, 0)	
	Chan	Fang	Chan	Fang
5	57.4163	72.9717	70.7447	87.4013
10	52.0454	74.5029	65.3847	72.1094
15	44.4295	66.2436	58.2968	61.3178
20	33.3746	55.9329	50.4419	57.6682
25	27.8228	40.2203	42.8607	46.4922

As observed from Table 4, the RMSE values consistently decrease as the sensor altitude increases for target locations at origin and (40, 60, 0) km and for both algorithms. The first case provides insight into how localization performs when the target is relatively close to the airborne sensor network, while the second case, with the target located at (40, 60, 0) km, demonstrates how increasing distance impacts accuracy.

In both scenarios, the minimum RMSE occurs at 20 km altitude, which corresponds to the upper altitude limit of typical airborne platforms used for surveillance and electronic warfare.

d. Altitude-based MLE–Monte Carlo CRLB Analysis

To further strengthen the altitude-dependent accuracy evaluation, a Maximum Likelihood Estimation (MLE) framework was implemented using Monte Carlo simulations for the same triangular sensor geometry. In this setup, 10 ns Gaussian timing noise was added to the TDOA measurements, and each altitude configuration was simulated over multiple independent trials to capture statistical consistency. The Monte Carlo approach ensures that the observed variations in localization performance are not due to random noise realizations but reflect genuine geometric and altitude-dependent effects.

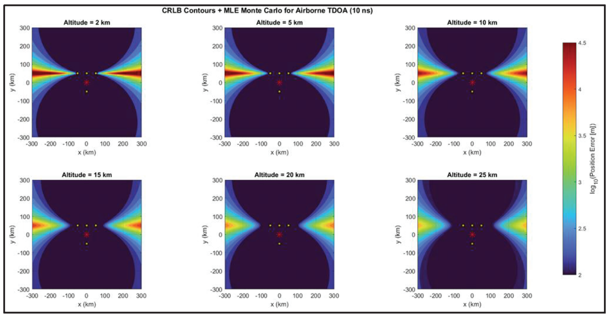

Fig.4: CRLB-Based Localization Accuracy for triangular flying formation using MLE and Monte Carlo trials

Figure 4 presents the corresponding CRLB-based error contours generated from the Monte Carlo–averaged MLE estimates at different sensor altitudes. Each subplot illustrates the spatial distribution of the theoretical lower bound on position error, offering a visual representation of achievable localization precision. As the altitude increases, the contour regions gradually broaden, indicating that higher altitudes reduce geometric diversity and, consequently, the attainable accuracy. This analysis confirms that the MLE–Monte Carlo outcomes align well with the CRLB trends, validating the robustness of the proposed simulation framework and reinforcing the earlier RMSE observations.

e. Number of sensors based analysis

The localization precision in a TDOA system improves as the number of sensors increases. A larger sensor network provides better spatial geometry and additional independent time-difference measurements, leading to reduced uncertainty in the estimated target position. The CRLB contour plots clearly illustrate that higher sensor counts yield tighter error bounds and lower RMSE values, demonstrating enhanced robustness and estimation accuracy for the airborne configuration at an altitude of 25 km.

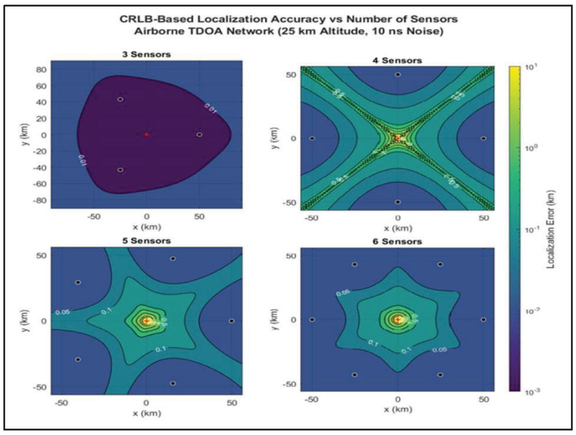

Fig 5: CRLB-based localization error contours for varying numbers of sensors in an airborne TDOA network at 25 km altitude with 10 ns timing noise.

The contour plots in Fig. 5 depict the CRLB-based localization accuracy for varying numbers of sensors in an airborne TDOA network. As observed, increasing the number of sensors from three to six significantly sharpens the error contours near the target, indicating reduced estimation uncertainty. The improvement is particularly noticeable beyond four sensors, where the error region becomes more confined and symmetric, reflecting enhanced geometric diversity and better dilution of precision in the multilateration process.

f. Spacing between sensor contour plot analysis

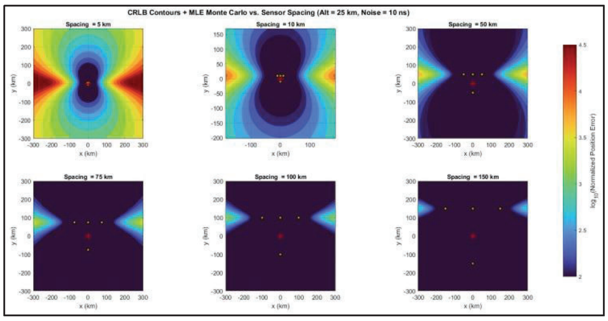

Fig.6: *CRLB contour plots showing the effect of sensor spacing on TDOA localization accuracy (altitude = 25 km, noise = 10 ns).*

The figure illustrates the variation in localization accuracy as a function of sensor spacing for a system of four TDOA sensors positioned in a triangular geometry at an altitude of 25 km. Each subplot represents a different inter-sensor spacing, ranging from 5 km to 150 km. The color contours correspond to the logarithmic scale of the normalized position error derived from the Cramér–Rao Lower Bound (CRLB), while the red star marks the true target position and yellow stars indicate the sensor locations. As the spacing increases, the localization geometry improves initially, reducing the overlapping hyperbolic regions and enhancing position estimation accuracy.

Beyond a certain separation distance, however, the improvement saturates, and the coverage region begins to degrade due to increased dilution of precision. This trend signifies the trade-off between spatial separation and measurement geometry — too small spacing leads to poor triangulation, while excessive spacing causes loss of sensitivity near the target area. The plots thus highlight the importance of optimizing sensor deployment to achieve a balance between geometric diversity and localization precision in practical TDOA systems.

V. CONCLUSION

Work presents a 3D-TDOA localization analysis using airborne sensor networks for geolocation of a stationary ground-based emitter. Among the implemented non-iterative algorithms, the Chan-Ho method exhibited marginally better accuracy than the Fang method, owing to its efficient closed-form linearization. Performance was evaluated using RMSE and GDOP, revealing that sensor geometry significantly influences localization accuracy. Triangular and square layouts outperformed others, with the triangular configuration selected for further analysis due to its slightly better error performance.

The study also examined the effect of sensor altitude and quantity on localization. Results showed that increasing altitude improves accuracy, with the best performance observed at 20 km when the emitter is within the coverage area. Additionally, adding more sensors reduced error, highlighting the benefits of spatial diversity. These findings contribute toward optimizing sensor deployment and algorithm selection in airborne TDOA systems for defense and surveillance applications.

REFERENCES

[1] S. Agrawal and M. Barshikar, "Enhanced Target Localization Using Time Difference of Arrival with Multiple Sensors," 2025 IEEE Space, Aerospace and Defence Conference (SPACE), Bangalore, India, 2025, pp. 1-5, doi: 10.1109/SPACE65882.2025.11170501.

[2] *H. Halevi, I. Bergel* and Y. Noam, "Asymptotic Performance of TDOA Estimation Using Satellites," in IEEE Transactions on Signal Processing, vol. 70, pp. 2349-2361, 2022, doi: 10.1109/TSP.2022.3169271.

[3] I. O. Tovkach, et al, "Analysis of Influence of Number of Sensors on Accuracy of Radio Source Position Determination Based on TDOA-, RSS- and AOA- Measurements," 2021 IEEE 3rd Ukraine Conference on Electrical and Computer Engineering (UKRCON), Lviv, Ukraine, 2021, pp. 217-220, doi: 10.1109/UKRCON53503.2021.9575365.

[4] M. Nemati, T. Baykas and J. Choi, "Performance of TDOA and AOA Localization Techniques for Different Base-Stations Topologies," 2019 13th International Conference on Signal Processing and Communication Systems (ICSPCS), Gold Coast, QLD, Australia, 2019, pp. 1-7, doi: 10.1109/ICSPCS47537.2019.9008716.

[5] S. Ergut, et al, "Localization via TDOA in a UWB Sensor Network using Neural Networks," 2008 IEEE International Conference on Communications, Beijing, China, 2008, pp. 2398-2403, doi: 10.1109/ICC.2008.456.

[6] Y. T. Chan and K. C. Ho, "A simple and efficient estimator for hyperbolic location," in IEEE Transactions on Signal Processing, vol. 42, no. 8, pp. 1905-1915, Aug. 1994, doi: 10.1109/78.301830.

[7] Guowei Shen, et al. "Performance comparison of TOA and TDOA based location estimation algorithms in LOS environment," 2008 5th Workshop on Positioning, Navigation and Communication, Hannover, Germany, 2008, pp. 71-78, doi: 10.1109/WPNC.2008.4510359.

[8] Y. Lin, Q. Chen, H. Zhang, Y. Ma, W. Zeng, G. Wei, H. Wang, and M. Xiao, "Design and test of a positioning system for a greenhouse electric micro-tiller based on ultra-wideband," *Mechanical Sciences*, vol. 13, pp. 225-236, Mar. 2022, doi: 10.5194/ms-13-225-2022.

[9] J. Pospisil, R. Fujdiak, and K. Mikhaylov, "Investigation of the Performance_of TDoA Based Localization over LoRaWAN Theory and Practice," Sensors, vol. 20, no. 19, p. 5464, 2020, doi: 10.3390/s20195464.

[10] M. Oussalah and H. Li, "TDOA Wireless Localization Comparison Influence of Network Topology", *DAFS*, vol. 2, no. 5, pp. 104–115, Nov. 2014.

[11] M. Delcourt and J.-Y. Le Boudec, "TDOA source-localization technique robust to time-synchronization attacks," *IEEE Trans. Inf. Forensics Secur.*, vol. 16, pp. 4249–4264, 2021.

[12] X. Pei, L. Li, X. Yang, and F. Guo, "A closed-form solution for source localization using FDOA measurements only," *IEEE Commun. Lett.*, vol. 27, no. 1, pp. 115–119, 2023.

[13] Z. Dai, et al, "Nearly optimal sensor selection for TDOA-based source localization in wireless sensor networks," *IEEE Trans. Veh. Technol.*, vol. 69, no. 10, pp. 12031–12042, 2020.

[14] J. Pan, "Multi-station TDOA localization method based on Tikhonov regularization," in *Proc. 7th Int. Conf. Intelligent Computing and Signal Processing (ICSP)*, 2022, pp. 1903–1906.

[15] S. Ivanov, et al, "RSS/TDOA-based source localization in microwave UWB sensor networks using two anchor nodes," *Sensors*, vol. 22, no. 8, p. 3018, 2022